

See discussions, stats, and author profiles for this publication at: <https://www.researchgate.net/publication/256758350>

1-Hydroxy-2-naphthaldehyde: A prospective excited-state intramolecular proton transfer (ESIPT) probe with multi-faceted applications

ARTICLE in JOURNAL OF LUMINESCENCE · AUGUST 2012

Impact Factor: 2.72 · DOI: 10.1016/j.jlumin.2012.03.036

CITATIONS

11

READS

49

2 AUTHORS, INCLUDING:



Bijan Kumar Paul

Indian Institute of Science Education and R...

72 PUBLICATIONS 895 CITATIONS

[SEE PROFILE](#)



Review

1-Hydroxy-2-naphthaldehyde: A prospective excited-state intramolecular proton transfer (ESIPT) probe with multi-faceted applications

Bijan Kumar Paul, Nikhil Guchhait*

Department of Chemistry, University of Calcutta, 92 A. P. C. Road, Calcutta-700009, India

ARTICLE INFO

Article history:

Received 12 December 2011

Received in revised form

10 February 2012

Accepted 8 March 2012

Available online 30 March 2012

Keywords:

1-Hydroxy-2-naphthaldehyde

ESIPT

Proteins

Micelles

Cyclodextrins

Liposomes

ABSTRACT

The present account aims at amassing and recounting on our series of spectroscopic studies with a potential excited state intramolecular proton transfer (ESIPT) probe 1-hydroxy-2-naphthaldehyde (HN12). After a detailed investigation from experimental as well as theoretical viewpoints, a deeper insight into the photophysics of the selected molecular system is provided from thorough spectral deciphering of the effects of solvent, medium pH and temperature. In the following sections, the ESIPT emission of HN12 has been documented to be a potential avenue wherefrom characterization of a wide variety of biological, biomimetic and supramolecular assemblies has been executed to commendable fruition. Efforts are also invested to delineate the location, distribution and strength of interaction of the probe with various microheterogeneous environments.

© 2012 Elsevier B.V. All rights reserved.

Contents

1. Introduction	2194
2. Photophysics of HN12	2195
2.1. Ground and excited state photophysics of HN12: solvent and pH effects	2195
2.2. Temperature effect studies	2197
2.3. Theoretical studies	2198
3. Photophysics of HN12 in various microheterogeneous environments	2198
3.1. Exploration of the microenvironments of biological system	2198
3.1.1. HN12 in protein cavity	2198
3.1.2. HN12 as an extrinsic reporter in exploring the unfolded and refolded states of a transport protein	2201
3.2. HN12 in nanocavities and biomimetic environments	2202
3.3. Photophysics and dynamics of HN12 in liposome membranes	2203
3.4. Wavelength-sensitive fluorescence behavior of HN12: the red-edge excitation	2206
4. Summary and conclusion	2207
Acknowledgments	2207
References	2207

1. Introduction

Research in the field of photochemistry has traditionally been a subject of elating fascination to the scientific world as because of the profusely modulated photophysics and photochemistry of

compounds sprouting through their photoexcitation, which has eventually led to the discovery of some interesting phenomena like excited state proton transfer (ESIPT or ESP) [1–4], charge transfer (CT) [5–8], electron transfer (ET) [9,10], conformational transformations such as isomerization [11,12], resonance energy transfer (FRET) [13–16] and so forth. With the progress of time, all these phenomena have enormously matured through the mammoth volume of works inclined along these directions and have eventually constructed some indispensable building blocks of

* Corresponding author. Fax: +91 33 2351 9755.

E-mail address: nguchhait@yahoo.com (N. Guchhait).

photochemistry. The ever-burgeoning interest in studying these excited state phenomena has fathomed much deeper with their successful implementation on a wide arena of applicative research.

Of all the elementary photoinduced phenomena observed in nature one of the most encountered one and of particular interest of the present review is the excited-state intramolecular proton transfer (ESIPT) reaction. The pioneering work of Weller [1] in the middle of the last century envisaged a new arena of research in the field of photochemistry out of the unique observation of ESIPT reaction in methylsalicylate. Since then a great deal of research has been devoted to the study of photoinduced proton transfer process along intramolecular hydrogen bonds (IMHBs) both in condensed phase and in gas phase and supersonic jets [17–25]. The photophysics of intramolecular hydrogen bonds in aromatic systems has captured special attention because of its essential role for the functionality of so-called photostabilizers [26,27], which are in wide technical use for the protection of organic polymers against degradation by the UV components of sunlight [28,29]. The four-level photophysical scheme of proton transfer (PT) reaction promotes its application as proton transfer lasers [30,31], UV filters [32], and facilitates its use as probes for investigating various biological and biomimicking environments [33–40]. Thus naturally, ESIPT systems seem to be a very promising

and splendid avenue for realization of some long-standing prospects. Such vast range of application has enormously contributed in making the study of this unique photoinduced phenomenon of ESIPT an active and dynamic subject of research even today. However, despite numerous efforts devoted since Weller [1], the phenomenon still continues to throw challenges both theoretically and experimentally. This is primarily because of the inherently complicated physical (e.g., quantum nature) and chemical (cleavage and formation of H-bond and subsequent nuclear rearrangement with inversion in the thermodynamic stability) nature of the process [23]. Such complexities have always acted in the direction of supplying immense fuel to the study of ESIPT process even in some of very simple and prototype systems. 1-Hydroxy-2-naphthaldehyde (HN12) is one of such simple systems belonging to the prototype family of *o*-hydroxybenzaldehyde that exhibits ESIPT emission following an electronic excitation. The present account aims at fabricating a unified picture of the photophysical events carried out with the molecule HN12. The following discussions will recast light on the photophysics of HN12 [41] and exploration of its caliber to inspect various biological and biomimicking microheterogeneous environments and different supramolecular assemblies [42–45]. We believe that the unified picture of the photophysics of HN12 and its modulations under a wide range of circumstances will provide a unique view to its potential usefulness as a fluorescent probe, apart from understanding of the fundamental phenomenon of ESIPT reaction. Details can be availed from the original contributions [42–45].

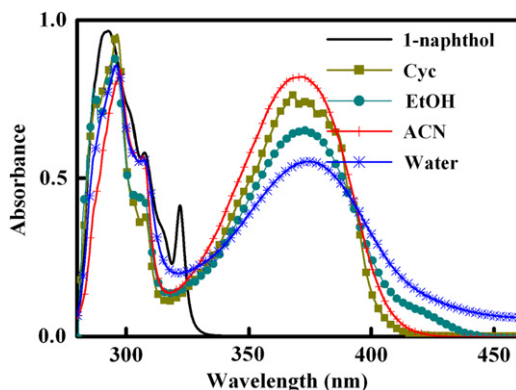
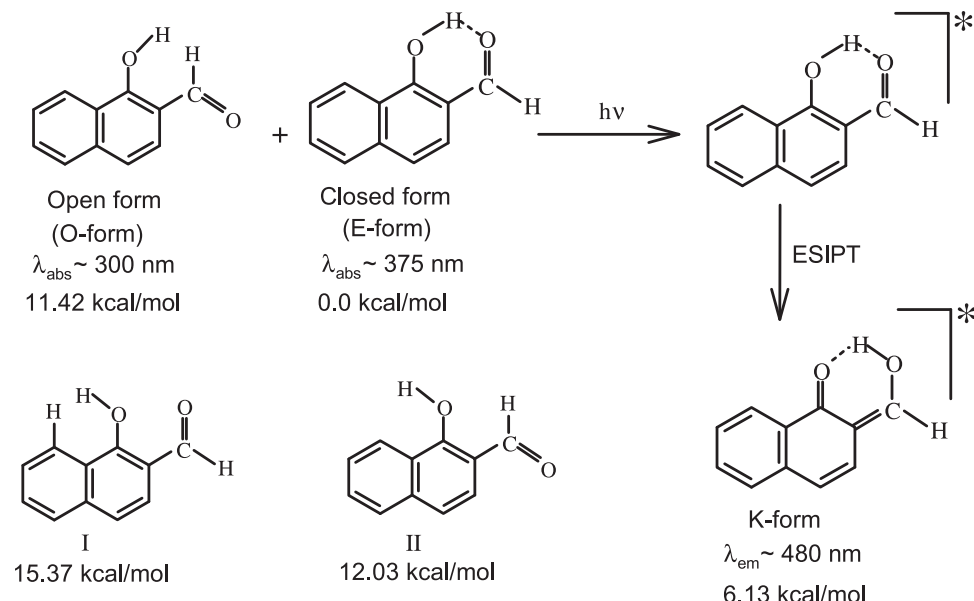


Fig. 1. Absorption spectra of HN12 in different solvents as indicated in the figure legend. The absorption spectrum of 1-naphthol in EtOH is also included for comparison.

2. Photophysics of HN12

2.1. Ground and excited state photophysics of HN12: solvent and pH effects

A detailed spectroscopic investigation on the photophysics of HN12 reveals that the molecule exhibits two strong absorption bands at ~300 and ~375 nm in all types of solvents (nonpolar, polar aprotic and protic) at room temperature (Fig. 1) [41]. A direct analogy with similar reported systems has led us to assign the lower energy band to the intramolecularly hydrogen bonded closed conformer (E-form) of HN12 (**Scheme 1**) while the higher energy band being responsible for the open conformer (O-form, **Scheme 1**). An attempt



Scheme 1. Schematic of the ESIPT process observed in HN12. Energies (calculated at DFT/B3LYP/6-31G(d,p) level of theory) of different conformers are given with respect to that of the E-form.

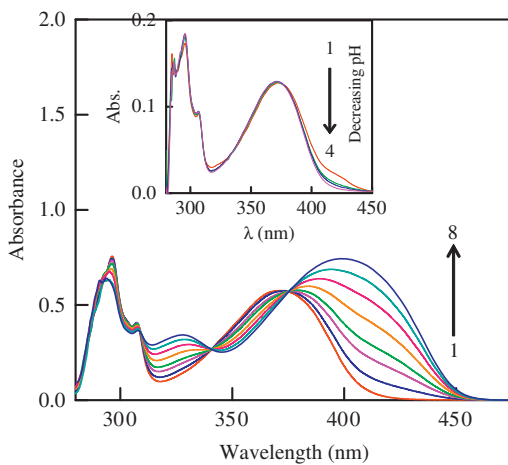


Fig. 2. Modulation of absorption spectral profile of HN12 in EtOH as a function of added base triethylamine (TEA). Direction of arrow indicates increasing concentration of base (TEA). Inset shows the effect of addition of acid (H_2SO_4) on the absorption profile of HN12 in EtOH.

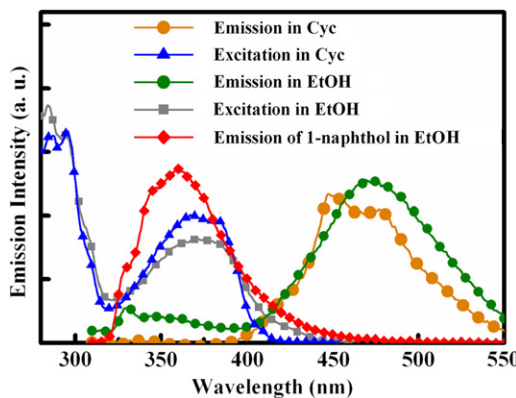


Fig. 3. Fluorescence emission ($\lambda_{\text{ex}}=300 \text{ nm}$) and excitation spectra ($\lambda_{\text{monitored}}=\lambda_{\text{em}}^{\max}$) of HN12 in various solvents as specified in the figure legend. The emission spectrum of 1-naphthalol in EtOH is also given for comparison.

to further scrutinize the solvent effect on the ground state properties of the molecule revealed an interesting observation in form of generation of a new hump at the long wavelength tail of the spectrum ($\sim 428 \text{ nm}$) in protic solvents (Fig. 1). This implies the possibility of formation of ground state intermolecular H-bonded ($\text{I}_{\text{e},\text{MHB}}$) solute–solvent clusters [20,21,41]. As far as the effect of pH variation on spectral properties are considered, addition of electron donor base triethylamine (TEA) to an ethanolic solution of HN12 is found to result in development of a new absorption band at $\sim 400 \text{ nm}$ by merging of ~ 428 and $\sim 375 \text{ nm}$ bands due to the generated anion of HN12. An equilibrium between the closed conformer of HN12 ($\lambda_{\text{abs}}\sim 375 \text{ nm}$) and its anion ($\lambda_{\text{abs}}\sim 400 \text{ nm}$) is indicated by the isosbestic point at $\sim 375 \text{ nm}$. A similar equilibrium between the open conformer ($\lambda_{\text{abs}}\sim 300 \text{ nm}$) and its anion ($\lambda_{\text{abs}}\sim 325 \text{ nm}$) is also pointed out by another isosbestic point at $\sim 340 \text{ nm}$ (Fig. 2). A decrement of the pH of the medium with addition of acid H_2SO_4 is found to result in suppression of the $\sim 428 \text{ nm}$ band probably owing to rupture of the intermolecular H-bonded clusters (inset of Fig. 2). However, that the variation of medium pH exerts no noticeable effects on the absorption spectral properties of HN12 in nonpolar solvents seems to be a reflection of the appreciable strength of the IMHB in nonpolar solvents.

As shown in Fig. 3, HN12 exhibits a large Stokes shifted fluorescence band at $\sim 475 \text{ nm}$ in all solvents ($\lambda_{\text{ex}}=300 \text{ nm}$). It is to note in this context that the principal absorption band of the E-form peaks at

$\lambda_{\text{abs}}\sim 375 \text{ nm}$ while the band at $\sim 300 \text{ nm}$ is attributed to the O-form (Scheme 1), nevertheless that excitation at $\lambda_{\text{ex}}=300 \text{ nm}$ yields the emission from the proton transferred tautomer (K-form) is not surprising because the E-form can also absorb in the region around 300 nm and thereby producing the large Stokes shifted emission of the K-form, while at the same time it is not unlikely that that excitation at the higher energy band ($\lambda_{\text{abs}}\sim 300 \text{ nm}$) might result in a rapid photoisomerization of the O-form to the E-form followed by subsequent proton transfer process in the excited state. The intramolecularly hydrogen bonded closed conformer on excitation undergoes photoinduced enol-keto tautomerism across the pre-existing IMHB and shows a red shifted emission band at $\sim 475 \text{ nm}$ for the keto tautomer (K-form of Scheme 1). In aqueous medium, the red shifted emission band is composed of both the keto-form and the hydrated clusters and hence, the band shifts slightly to the red ($\sim 488 \text{ nm}$). In nonpolar hydrocarbon solvents, for example, in cyclohexane, HN12 shows a broad structured emission band at $\sim 475 \text{ nm}$ with a hump at $\sim 430 \text{ nm}$ ($\lambda_{\text{ex}}=300 \text{ nm}$). In other nonpolar and polar aprotic solvents, apart from the emission band at 475 nm , another band at $\sim 350 \text{ nm}$ is observed due to emission from the open unsolvated form which absorbs at $\sim 300 \text{ nm}$ [41]. The three emitting species are thus identified as (i) intramolecularly hydrogen bonded closed conformer ($\lambda_{\text{em}}\sim 475 \text{ nm}$), (ii) open conformer ($\lambda_{\text{em}}\sim 350 \text{ nm}$) and (iii) intermolecularly hydrogen bonded species ($\lambda_{\text{em}}\sim 480 \text{ nm}$) (Fig. 3). Due to small change in dipole moment of the emitting species compared to that of the ground state species (calculated dipole moment of E-form=3.07 D and of

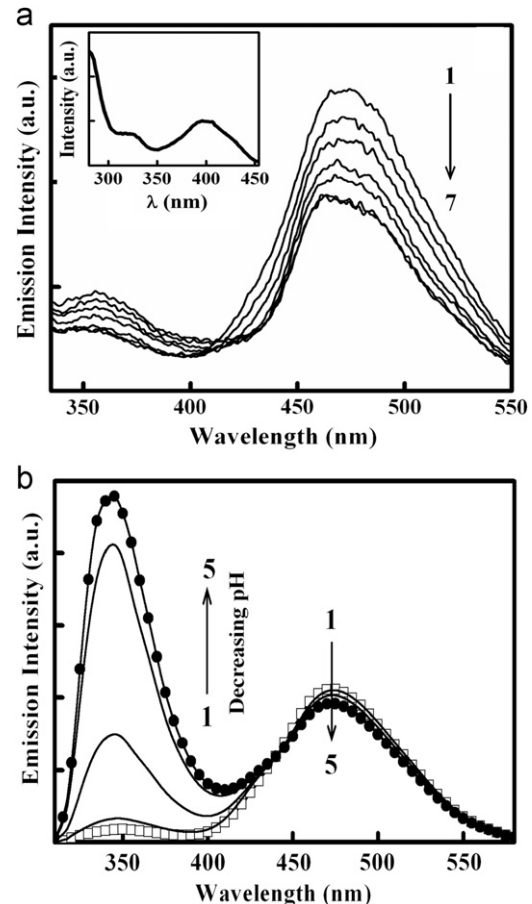


Fig. 4. (a) Modulation of emission spectral profile of HN12 in EtOH as a function of added base triethylamine (TEA). Direction of arrow indicates increasing concentration of base (TEA). Inset shows the excitation spectrum of HN12 in EtOH ($\lambda_{\text{monitored}}=\lambda_{\text{em}}^{\max}$) in the presence of TEA. (b) Effect of addition of acid (H_2SO_4) on the emission profile of HN12 in EtOH.

Table 1

Comparison of the photophysical properties of various conformations of HN12.

HN12 conformation	λ_{abs} (nm)	λ_{em} (nm)
O-form	~300	~350
E-form	~375	~475–488
Anion of O-form	~325	~360
Anion of E-form	~400	~460

K-form = 2.63 D (at DFT/B3LYP/6-31 G(d,p) level of calculation) [41], the position of the red shifted band remains almost inert to the variation of solvent polarity. That the excitation spectra (Fig. 3) obtained in all solvents assayed juxtapose well with the corresponding absorption spectra indicates that the origin of the tautomer (K-form) emission is through excitation of the E-form.

In order to assess the pH effect on the excited state photophysics of HN12, pH variation experiments were performed on the emission profile which led to the observation of blue shift of the emission maxima of the lower energy band (~475 nm) upto ~460 nm and a slight red shift of the higher energy band from ~350 to ~360 nm upon addition of TEA to an ethanolic solution of HN12 (Fig. 4a). Nice corroboration of the excitation spectra of HN12 in the presence of TEA with the absorption spectra under similar experimental conditions confirms the formation of anion of the E (~460 nm) and O-forms (~360 nm) of HN12 upon treatment with a base [41]. Similarly, a decrement of pH was found to result in remarkable intensity enhancement of the higher energy band (~350 nm) with concomitant depletion of the same at the lower energy band (~475 nm) but to a much lesser extent (Fig. 4b). These observations are connected to the rupture of solute–solvent I_rMHBs. Decreasing the pH of nonpolar solutions of HN12 also produced similar results [41]. However, at sufficiently low pH in nonpolar solvents, the intensity corresponding to the excited keto form is considerably reduced with marked enhancement of that of the O-form. A possible explanation is that a sufficiently low pH may induce the formation of cationic species of HN12 (protonation), which will consequently restrict the operation of ESIPT leaving only the band of the O-form [20,21]. In order to enable a visual comparison of the discernible differences of the photophysical properties among the various conformations of HN12 the characteristic absorption and emission wavelengths of its different conformations are appended in Table 1.

Operation of an ultrafast ESIPT process in HN12 has also been afforded by further support from fluorescence lifetime measurements which conform to a virtually barrierless process of proton translocation along the excited state potential energy surface (PES). Also relatively longer lifetime of the K-form in aprotic solvents compared to those in protic media suggests the active role of nonradiative deactivation channels in protic solvents operating probably via the existing I_rMHBs [20,21,41].

2.2. Temperature effect studies

The excited state photophysics of HN12 has been found to be remarkably sensitive towards the variation of temperature of the medium both in nonpolar and polar solvents. In nonpolar solvent (cyclohexane) the rise of temperature has been found to exert its effect in terms of decreasing intensity of the ~475 nm band (K-form) with simultaneous slight increment of intensity of the ~350 nm band. Such an observation may originate from two effects, viz., (i) rise of temperature induces rupture of IMHB—a direct manifestation of which is in attenuation of emission of the K*-form and enhancement of the same of the O*-form; (ii) activation of nonradiative deactivation channels with temperature leading to decrease of fluorescence. The present observation seems to be the result of interplay of both the

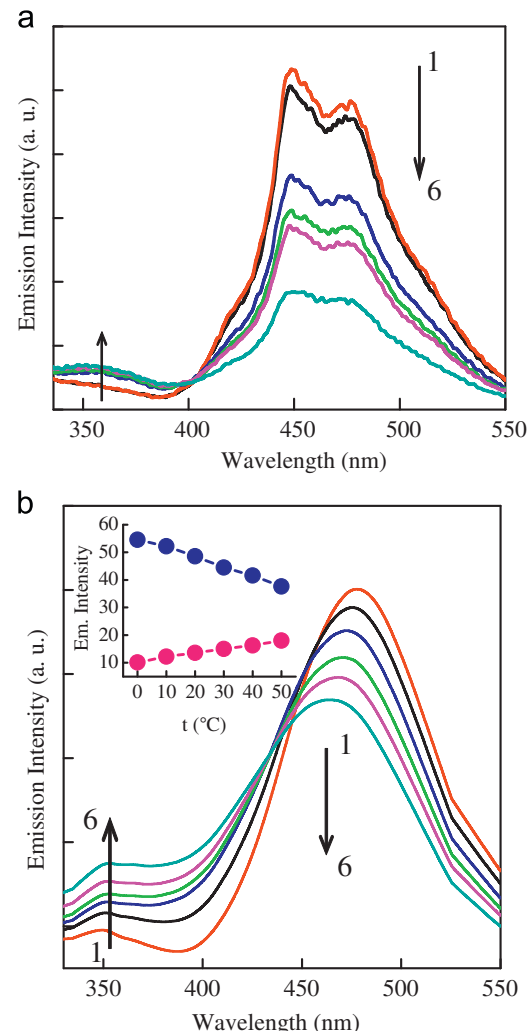


Fig. 5. Effect of temperature on the emission profile ($\lambda_{\text{ex}}=300$ nm) of HN12 in (a) cyclohexane and (b) EtOH solvents. Curves 1–6 correspond to $t=0, 10, 20, 30, 40, 50$ °C. Inset shows the variation of tautomer emission intensity (blue) at $\lambda_{\text{em}} \approx 480$ nm and the open conformer emission intensity (pink) at $\lambda_{\text{em}} \approx 353$ nm as a function of temperature. (For interpretation of the references to color in this figure legend, the reader is referred to the web version of this article.)

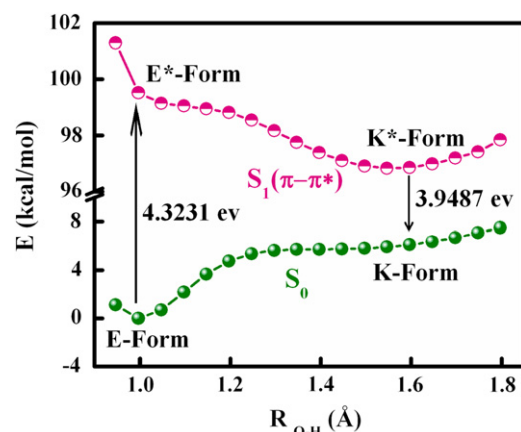


Fig. 6. Theoretically calculated potential energy curve (PEC) for the ESIPT reaction in HN12. Plot of variation of energy (E in kcal/mol) as a function of the PT reaction coordinate (O–H distance in Å) for the ground (S_0) and the excited (S_1) states. Calculations at B3LYP/6-31G(d,p) level for the S_0 -state and TD-B3LYP/6-31G(d,p) level for the S_1 -state.

effects. In protic solvent (EtOH), the same effect is reproduced with an additional observation of blue shift of the ~475 nm band with temperature indicating the possibility of formation of unsolvated structures which are energetically less stable than the solvated counterparts (Fig. 5). This proposition receives further support from the theoretical calculation showing a greater stability of the solvated structure in EtOH (using polarizable continuum model (PCM) at DFT//B3LYP/6-31 G^{**} level of theory) by ~8 kcal/mol than the unsolvated one. The presence of isoemissive point (~402 nm) between the two bands (K-form and O-form) in cyclohexane indicates an equilibrium between the two species and that interconversion between them is possible through proper variation of temperature.

2.3. Theoretical studies

Quantum chemical calculations have been performed on HN12 with a view to achieve a theoretical insight into its photophysics with particular emphasis being inclined along (i) structure and stability of different conformations of HN12, (ii) ESIPT reaction and (iii) strength of IMHB. The conformational landscapes of HN12 molecule are explored in the electronic ground state by density functional theory (DFT) method using B3LYP hybrid functional and 6-31G^{**} basis set [26,46–49]. Calculations predict the closed E-form to be the most stable conformer at the ground state as realized from the presence of stabilizing IMHB, the lack of which destabilizes the O-form (Scheme 1). Another destabilizing influence viz., Peri-interaction between H of OH and H₈ of naphthalene nucleus is invoked to account for the additional instability of other open conformers (I and II in Scheme 1).

The occurrence of ESIPT in HN12 can be most critically assessed by elucidation of the PES along the reaction coordinates. The purpose has been accomplished according to “distinguished coordinate approach”, i.e. by observing the energy change with increasing O–H bond distance (R_{OH}) [17,18,20–23] and optimizing all other geometrical parameters at every choice of the OH distance. Fig. 6 depicts a more or less monotonic increase of energy at S₀ surface with increasing R_{OH}

distance whereby dictating the inoperativeness of a GSIPPT reaction through the repulsive nature of the GSIPPT curve, i.e. the E-form constitutes the global minimum at the S₀ surface. However, the nature of the S₁ surface (an asymmetric double well type potential) elegantly confirms to the experimental observation of ESIPT in HN12 through drastic reduction of barrier for E- to K-conversion along with their thermodynamic stability inversion. The process being practically barrierless is in line with the ultrafast fluorescence lifetime of the K-form [41].

Evaluation of the strength of IMHB (E_{IMHB}) is an important factor from the standpoint of photophysics of HN12. An energy difference between the E-form and the O-form/II-form gives E_{IMHB} to be, respectively ~11.4 and 15 kcal/mol. The difference in E_{IMHB} in the two cases is a reflection of the destabilization imparted by the Peri-interaction effect [41]. Experimentally E_{IMHB} in HN12 is found to be 7.62 kcal/mol as calculated according to the method described by Zhdorozhnyi and Ishchenko [50], i.e. the intramolecular hydrogen bond energy (E_{IMHB}) can be expressed through the relation:

$$\frac{\Delta v_{C=O}}{v_{C=O}} = -K_{C=O} E_{\text{IMHB}} \quad (1)$$

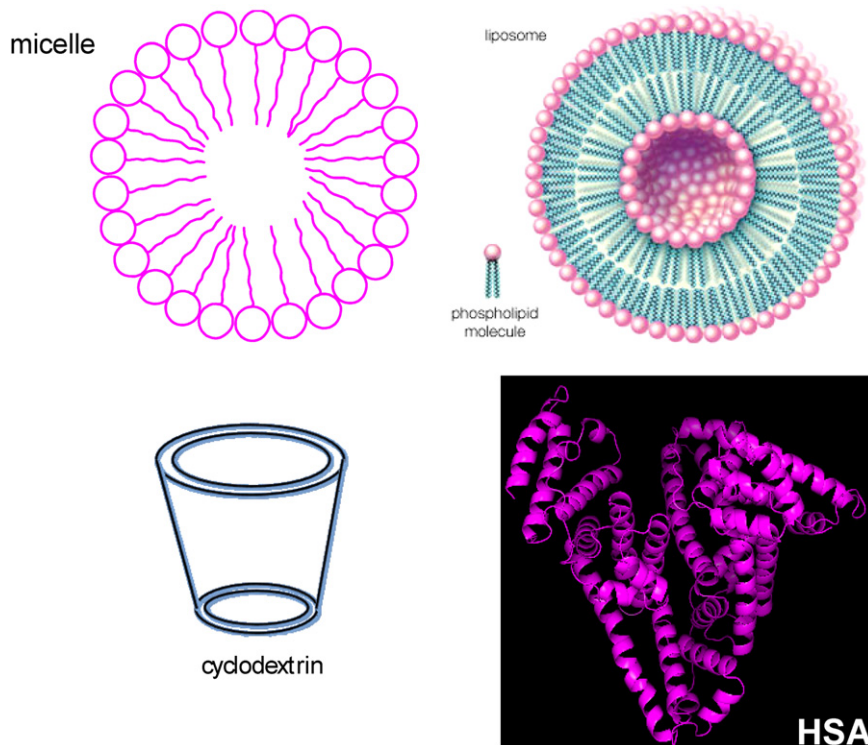
where $\Delta v_{C=O}$ and $K_{C=O}$ are the magnitudes of the spectral shift and proportionality constant coefficient, respectively (reported value of $K_{C=O} = 9.6 \times 10^{-4} \text{ mol } \text{kJ}^{-1}$) [50]. Acceptable agreement of the experimental value with the theoretically calculated one also justifies the choice of the theoretical methods adopted for calculations [50–52].

3. Photophysics of HN12 in various microheterogeneous environments

3.1. Exploration of the microenvironments of biological system

3.1.1. HN12 in protein cavity

In this section we recount the efficiency of HN12 to work as an extrinsic fluorescence molecular reporter to monitor the



Scheme 2. Simplified schematic structures of different supramolecular assemblies (micelle, liposome, cyclodextrin) and the protein HSA.

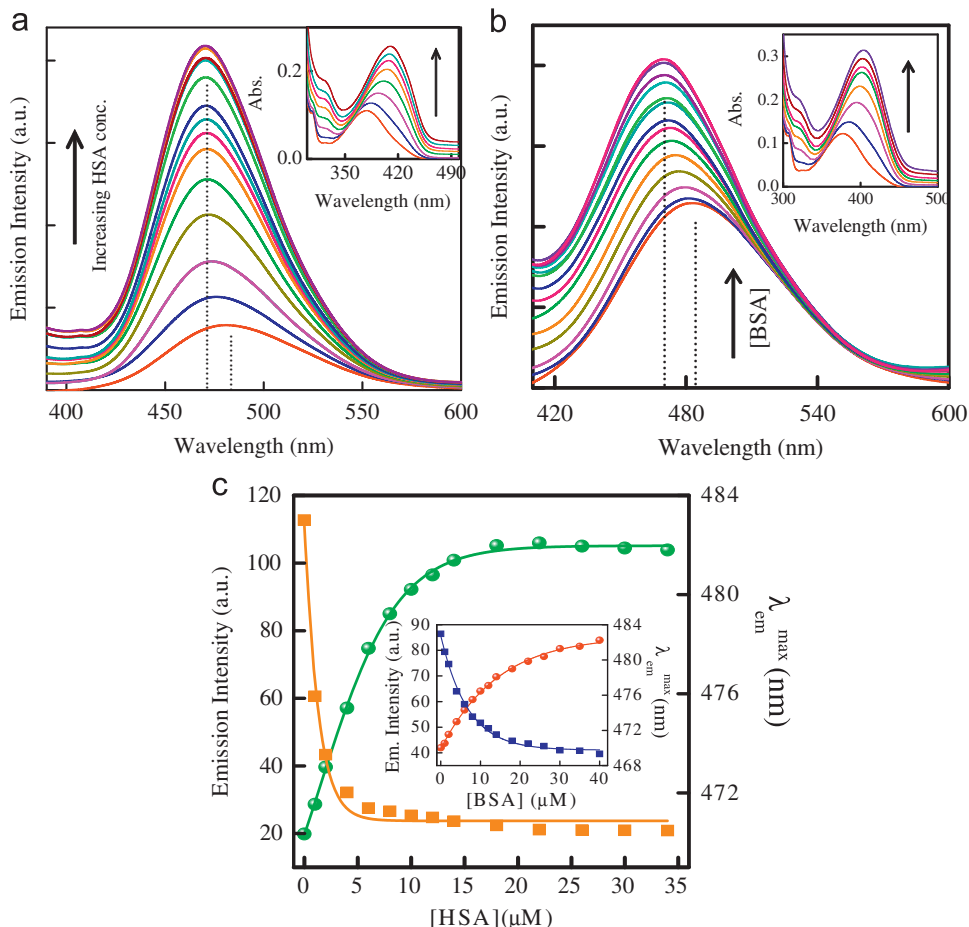


Fig. 7. (a) Modulation of absorption (inset) and emission ($\lambda_{\text{ex}}=375 \text{ nm}$) spectral profiles of HN12 as a function of increasing concentration of protein HSA. Curves 1 → 16 correspond to $[\text{HSA}]=0, 2, 4, 6, 8, 10, 12, 14, 18, 22, 26, 30, 33, 34, 35, 37 \mu\text{M}$. (b) Modulation of absorption (inset) and emission ($\lambda_{\text{ex}}=375 \text{ nm}$) spectral profiles of HN12 as a function of increasing concentration of protein BSA. Curves 1 → 14 correspond to $[\text{HSA}]=0, 2, 4, 6, 8, 10, 12, 14, 18, 22, 26, 30, 33, 34 \mu\text{M}$. (c) Variation of emission intensity at the PT emission band ($\lambda_{\text{em}}=480 \text{ nm}$) and $\lambda_{\text{em}}^{\max}$ (nm) of HN12 with increasing HSA concentration. Inset shows the effect with the protein BSA.

microheterogeneous media of a biological system viz. protein sample [42]. For this purpose we used the model transport proteins human serum albumin (HSA) and bovine serum albumin (BSA) (Scheme 2). The first indication of interaction of HN12 with HSA and BSA was manifested on the absorption profile through enhancement of absorbance with concomitant red shift of the maxima (inset of Fig. 7a and b) as a function of increasing serum albumin concentration. The most dramatic modulation of the photophysics of HN12 on being interacted with serum albumins, however, was reflected on the emission profile in the form of a remarkable intensity enhancement with simultaneous blue shift of the emission wavelength (Fig. 7a and b). Such spectral modifications were intertwined with the hindrance on rotational motion of the phototautomer (K-form) of HN12 in the protein:HN12 complexes. A direct comparison with the results of solvent effect on the emission profile (discussed in previous section) reveals that change in properties of solvent microenvironments of HN12 induces a shifting of its emission maxima, e.g., $\lambda_{\text{em}} \sim 475 \text{ nm}$ in nonpolar, nonhydrogen bonding solvent cyclohexane vs. $\lambda_{\text{em}} \sim 488 \text{ nm}$ in highly polar, hydrogen bonding aqueous medium. Thus the observed blue shift of emission maxima of HN12 with increasing protein concentration may reasonably be connected to the binding of the probe to some hydrophobic interior of protein backbone, a proposition that goes in line with the neutral and hydrophobic nature of HN12. Although it is rather more logical to entrust the blue shift on a conjugate effect of polarity and rigidity that jointly modify the

environment at immediate vicinity of the fluorophore furnishing the observed effects. Although the nature of interaction of HN12 with protein HSA and BSA is qualitatively same, but a close inspection of Fig. 7c pinpoints a differential behavior which is the requirement of lower concentration of HSA than BSA for the interaction to attain the saturation level. This reflects the higher motional restriction and stronger binding of the probe with HSA than BSA, as complemented from the estimated binding constants: $K_{\text{HN12}}^{\text{HSA}} = 1.23 \times 10^5$ and $K_{\text{HN12}}^{\text{BSA}} = 4.50 \times 10^4 \text{ M}^{-1}$ (binding constants are determined from Benesi-Hildebrand plot on the basis of emission intensity results [42]). Negative free energy change stands in support of spontaneous proceeding of the process of binding of HN12 with HSA and BSA ($\Delta G/\text{kJ mol}^{-1} = -29.13$ for HSA and -26.63 for BSA) [42]. These observations are strongly complemented from the steady state anisotropy measurements which exhibits a marked increase with increasing protein concentration followed by attainment of the saturation level indicating the rising degree of motional restrictions imparted on the probe and then marking the point of saturation of the effect (e.g., the fluorescence anisotropy (r) increases from 0.099 for HN12 in aqueous buffer to 0.264 in 30 μM HSA and 0.263 in 30 μM BSA) [42]. Steady state data and their interpretation were found to be concretized on the lexicon of time-domain experiment in terms of fluorescence lifetime measurements which reveals an enhancement with increasing protein concentration (average lifetime $\langle \tau_f \rangle = 0.055 \text{ ns}$ in aqueous buffer vs. $\langle \tau_f \rangle = 0.365 \text{ ns}$ in 40 μM HSA and $\langle \tau_f \rangle = 0.15 \text{ ns}$ in 40 μM BSA

[42]) as has been realized by the diminution of nonradiative decay rate constants (k_{nr}) inside the confined environment of protein backbone ($k_{nr}=17.67 \times 10^9 \text{ s}^{-1}$ in aqueous buffer vs. $k_{nr}=2.641 \times 10^9 \text{ s}^{-1}$ in 40 μM HSA and $k_{nr}=6.667 \times 10^9 \text{ s}^{-1}$ in 40 μM BSA [42]) [41,42,53–56].

Such significant modulation of the ESIPT photophysics of HN12 within the protein microheterogeneous environment invokes one's natural inquisition to delve into the influence of solvent microenvironment on the ESIPT process of the probe. Hence to pursue this inquest the following line of arguments has been espoused [45]. Considering the ultrafast nature of the ESIPT process in HN12, the enhancement of the rate of ESIPT within confined microheterogeneous environments can be excluded from being a probable reason of increment of the quantum yields of the tautomer emission of HN12, rather the responsible factor is the retardation of the rate of radiationless transition due to the spatial and hydrophobic interaction within the microheterogeneous assemblies. Roberts et al. [37] obtained similar results for inclusion complexes of 10-hydroxybenzo[*h*]quinoline in β -CD and γ -CD (CD abbreviates for cyclodextrin) and they interpreted the results in a similar manner. However, they did not address another possibility that can be debated. Although ESIPT is a very fast process and has no (or negligible) intrinsic barrier (*vide Section 2.3, Fig. 6*), it depends upon the properties of the solvent microenvironment. The solvent could play a crucial role in terms of introducing a “solvent-induced barrier” [57–60] to ESIPT reaction. The solvent induced barrier to ESIPT originates from the interaction of the normal (E-form) and tautomer (K-form, Scheme 1) dipole with the polarization of the surrounding solvent and is determined by solvent dielectric properties [58–60]. In the solvophobic interior (of proteins, cyclodextrins, micelles, etc.), the

“solvent induced barrier” to ESIPT decreases, favoring enhancement of the rate of ESIPT, resulting in enhanced tautomer emission in encapsulated state as rapid ESIPT outweighs the effect of competing non-radiative processes for the depopulation of photoexcited closed conformers (Scheme 1).

It is noteworthy that the solvent polarity/dielectric property may play a role in controlling the dynamics of ESIPT. It is well established that the hydrogen bonding property of solvent molecules perturbs ESIPT through external H-bonding interaction with the solute molecule and retards the ESIPT rate. For example, the phototautomers of (hydroxyphenyl)benzazoles due to ESIPT have been demonstrated to be more efficiently produced in dry hydrocarbon solvents as compared to alcohols or water due to less (or absence of) competition between intra- and intermolecular H-bonding with the solvent molecules [61,62]. Thus, the most important and predominant factor that contributes to the enhancement of tautomer emission of HN12 in confined microheterogeneous environments seems to be the lesser H-bonding interaction within the solvophobic interior (e.g., lesser degree of solute (HN12)-solvent intermolecular hydrogen bonding) rather than its less polar environment. The relevance of the present argument seems to be supported by the finding that the fluorescence yield (Φ_f) of HN12 undergoes a discernible enhancement on moving to nonpolar, non-hydrogen bonding solvents (e.g., $\Phi_f=0.014$ in cyclohexane, 0.012 in *n*-heptane) from polar protic medium (e.g., $\Phi_f=0.007$ in water, 0.008 in methanol) [45].

In probe–protein binding interaction studies knowledge of the probable binding location of small molecular probes within the microheterogeneous assembly of the protein is important. Herein, the blind docking simulation strategy has been applied to delineate the probable binding location of the probe HN12 in HSA (PDB ID: 1AO6 [63]). In order to evaluate an unbiased result in this

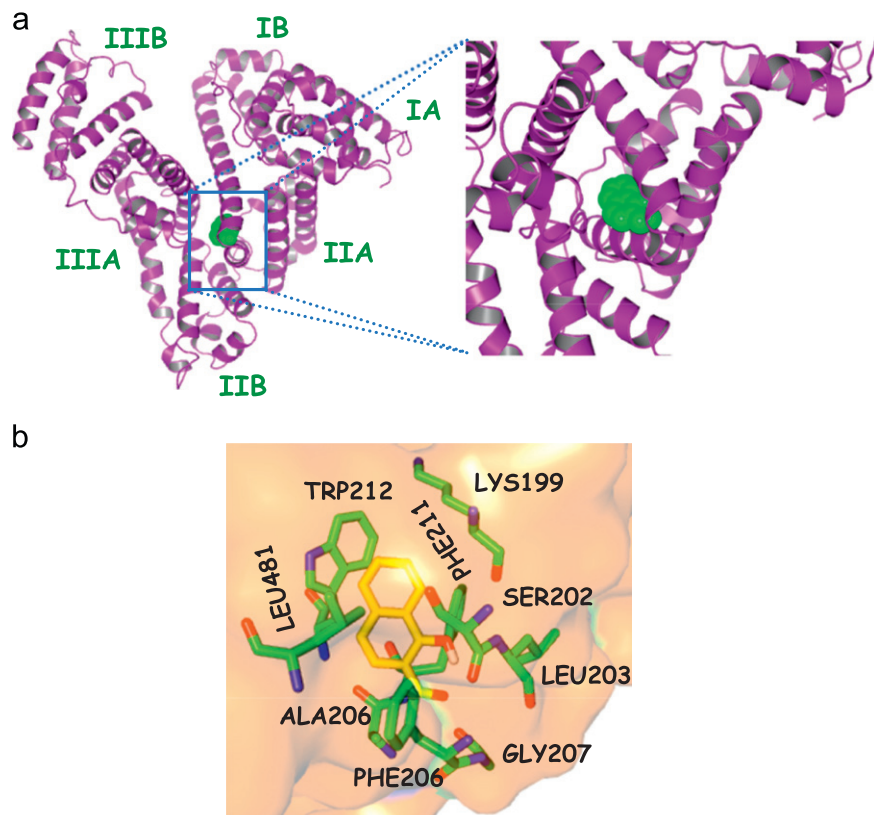


Fig. 8. (a) Stereo view of the docked conformation of the probe HN12 with the protein HSA. A magnified view at the site of interaction of HN12 is also shown. The probe HN12 is shown in Corey–Pauling–Koltun (CPK) model. Panel (b) displays the protein residues in near vicinity (within 5 Å) of HN12 over a molecular surface representation of the protein. Color scheme: blue for nitrogen atoms, red for oxygen atoms and carbon atoms are green for protein residues and yellow for the probe. Hydrogen atoms are omitted for reasons of clarity. (For interpretation of the references to color in this figure legend, the reader is referred to the web version of this article.)

respect, the AutoDock-based [64,65] blind docking simulation protocol has been employed as the actuating tool. The AutoDock-based blind docking technique includes a search over the entire surface of the protein for binding sites (and simultaneously optimizes the conformations of the peptides [66,67]) whereby indulging in an unbiased result, and hence has rightly been described as “very encouraging” in a recent review [67]. The stereo view of the minimum energy docked conformation displayed in Fig. 8a reveals hydrophobic subdomain IIA of the protein to be the favorable binding site for the probe molecule [42,54,55,68,69,103]. This observation is further substantiated by the fact that the principal hydrophobic binding sites in HSA are located in domains II and III, while domain I, characterized by a net negative charge, can serve as an appropriate binding site for cationic probe molecules [69]. The lowest binding energy conformer has been searched out of 10 different conformations for each docking simulation and the resultant minimum energy one has been exploited for further analysis. As is usual in a blind docking simulation protocol we obtained number of binding sites and the corresponding binding constants and free energies. Compelling evidence for probable binding location of HN12 in subdomain IIA of HSA has been derived from the observation that binding of HN12 in other binding pockets of BSA is characterized by unfavorable free energy change ($\Delta G > 0$). Whereas binding of HN12 in domain IIA is found to be characterized by a favorable binding energy of -5.59 kcal/mol along with a reasonably low magnitude of the inhibition constant i.e. $80.09 \mu\text{M}$. Also Fig. 8b indicates the protein residues in near vicinity (within 5 \AA) of the probe (e.g., Phe-211, Lys-199, Ser-202, Leu-481, Leu-203, Ala-206, Trp-212, Phe-206, Gly-207).

3.1.2. HN12 as an extrinsic reporter in exploring the unfolded and refolded states of a transport protein

After successful evaluation of the efficiency of HN12 as an external molecular reporter to study proteinaceous microenvironments [42] we intended to decipher the caliber of the selected molecular system in unraveling the characteristics and mechanism of chemical unfolding of protein by SDS and urea and also protective effect of SDS on urea-denatured protein [43]. These documents, however, happen to secure their positions among the very few examples in the literature of employing an ESIPT probe for the said purposes [53–56]. Research in the field of photobiology has witnessed an explosive evolution of works on the active topics of protein-protein and protein-surfactant interactions [70–73] of which the case of BSA-SDS interaction has been addressed and characterized by several researchers in different time utilizing various spectroscopic techniques [70–73]. It has been confirmed by Zaitsev et al. [74] and Gelamo et al. [75] that the interaction of BSA with SDS gives rise to appearance of four distinct regions in the binding isotherm recognized as—(i) region of specific binding (reflected in form of increasing α value which continues upto $\sim 0.1 \text{ mM}$ of total SDS concentration), (ii) region of non-cooperative binding (between 0.2 and 0.4 mM of total SDS concentration where the rise is slowed down), (iii) region of cooperative binding (showing its onset at $[\text{SDS}] \sim 0.6 \text{ mM}$), (iv) region of saturation binding (starting from $[\text{SDS}] \sim 5 \text{ mM}$ and wherefrom no further binding is operative). Here α , the fraction of BSA bound to SDS, is defined by the following equation:

$$\alpha = (I_{\text{obs}} - I_{\text{free}}) / (I_{\text{sat}} - I_{\text{free}}) \quad (2)$$

in which I_{obs} , I_{sat} and I_{free} are fluorescence intensities of Trp of BSA at any surfactant concentration, under saturation binding condition and in absence of surfactant, respectively [52,74]. We have demonstrated that the ESIPT emission of HN12 can serve as an excellent molecular reporter to follow the protein-surfactant interaction. The variation of the position of the PT band and in particular the emission intensity of the PT band of HN12 reflects

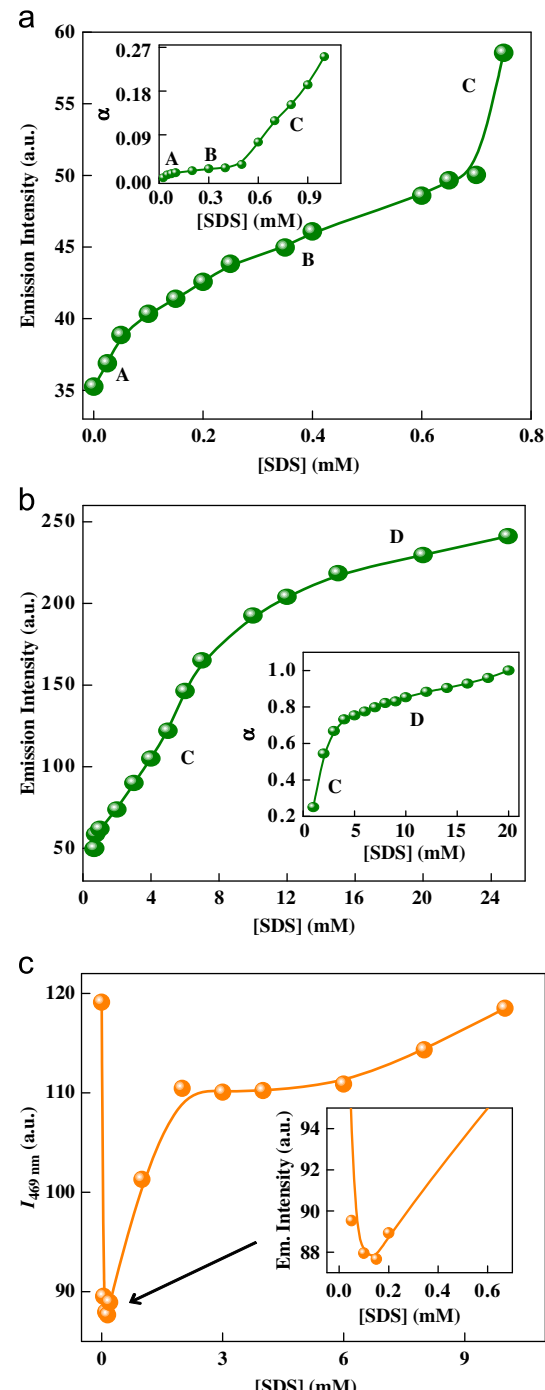


Fig. 9. Variation of PT emission intensity ($\lambda_{\text{em}}=480 \text{ nm}$) of HN12 in BSA as a function of SDS concentration. Range of SDS concentrations are: (a) 0 – 0.8 mM and (b) 0 – 25.0 mM . Insets show the binding curves corresponding to the interaction between BSA and SDS in terms of variation of α (fraction of BSA bound to SDS) against total SDS concentration (in mM). (c) Plot of variation of PT emission intensity ($\lambda_{\text{em}}=480 \text{ nm}$) of HN12 in urea (6 M)-denatured BSA as a function of total SDS concentration (in mM). All measurements are done with $[\text{BSA}] = 5 \mu\text{M}$ in Tris-HCl buffered condition.

the changes in hydrophobicity of respective microenvironments produced upon varying the SDS concentration in protein (BSA) medium. The spectral information obtained using HN12 as an external probe is authentic replication of the nature of protein-surfactant interaction obtained by monitoring the intrinsic tryptophan emission of BSA [74]. This is depicted in Fig. 9a and b. Another important aspect that has been clarified by the utilization

of the ESIPT emission of HN12 for mapping the renaturing action of SDS upon urea-denatured BSA. Helicity of the larger loop of BSA is retained to some extent in presence of SDS while it is completely ruptured in presence of a stronger denaturant urea. Addition of SDS to a urea-denatured BSA solution results in restoration of the lost helicity in the larger loop to the extent it is present in only SDS-denatured BSA. Fig. 9c reflects a distinct manifestation of these effects through consistent modulation of the PT emission intensity of HN12. Within the initial low concentration range of SDS, the PT emission intensity decreases and this continues up to 0.15 mM of [SDS], thereafter a sharp increase is followed by a region of constancy. The protective action of SDS at low concentration range leads to decrease in the availability of binding sites for the probe so that some of the probe molecules are expelled from specific binding sites of BSA upon addition of SDS due to their competitive binding nature. This extends up to $[SDS]=0.15$ mM causing intensity depletion of HN12, followed by a reverse effect (intensity enhancement) up to 2 mM of SDS when normal denaturing action of SDS comes into play. This observation also complies with earlier reports that protective action of SDS comes to fruition in low concentration range [70,71].

3.2. HN12 in nanocavities and biomimetic environments

Confinement of a molecule in a molecular pocket leads to significant modifications of its physical and chemical properties and thereby paves way for research from the view-point of characterizing the organized media as well as the probe molecule.

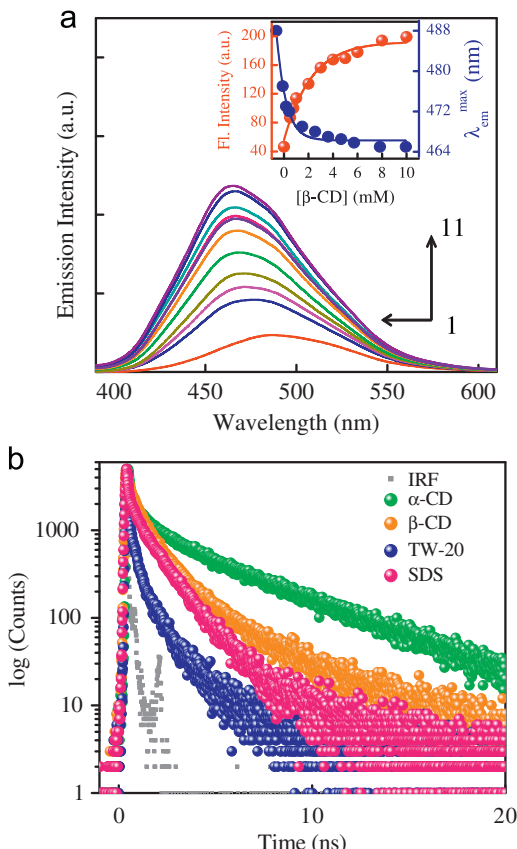


Fig. 10. (a) Emission profile ($\lambda_{ex}=375$ nm) of HN12 with increasing concentration of $\beta\text{-CD}$. Inset depicts the modulation of emission intensity at the PT emission band ($\lambda_{em}=480$ nm) and λ_{em}^{\max} (nm) of HN12 with increasing $\beta\text{-CD}$ concentration. (b) Representative time-resolved fluorescence decay profiles for HN12 in various supramolecular assemblies as indicated in the figure legend. $[CD]/[SDS]=10$ mM and $[TW-20]=100$ μM ; $\lambda_{ex}=375$ nm and $\lambda_{monitored}=460$ nm.

It reduces the degrees of freedom available to the molecule to move along reaction coordinates whereby making the system robust and effectively immune to perturbations from external agents. On this perspective, cyclodextrins and micelles (Scheme 2) are some of the well-known molecular assemblies that have long been utilized in the study of host-guest complexations. With a view to the ability of these inclusion complexes to serve as miniature models for studying the mode of action of enzymes [76,77], mimicking the reactions in biosystems [77,78] and so forth, their characterization has traditionally been a subject of profuse demand with brilliant future prospects [76–79]. Selection of appropriately sized molecular probe has been recognized as an efficient technique to study the thermodynamics and spectroscopy of host-guest complexations through the modulated photophysics of the probe as imparted by the organized media. This section is focused on the account of modulated photophysics of HN12 in different supramolecular assemblies provided by cyclodextrins (CDs) and micellar media.

Addition of CDs to an aqueous solution of HN12 was found to induce most dramatic modifications to its photophysics in terms of remarkable intensity enhancement accompanied with a slight blue shift to the emission profile (Fig. 10a) [45]. These observations, in analogy to our previous results for protein-HN12 interaction, are argued based on the idea of incorporation of the probe molecules inside hydrophobic CD-nanocavity. The stoichiometry of the complexes was found to depend on the nature and size of the host (CDs), e.g., the stoichiometry was 1:1 for β - and $\gamma\text{-CD}$, while it was 1:2 for HN12: $\alpha\text{-CD}$, as determined from Benesi-Hildebrand plot using the emission intensity data [45]. These observations were strongly complemented from the steady state anisotropy and fluorescence lifetime measurements which emerged to be remarkably higher for HN12: $\alpha\text{-CD}$ complex (Fig. 10b). The estimated binding constants form HN12:CD inclusion complex formation were: $K=6.86 \times 10^3 \text{ M}^{-2}$ with $\alpha\text{-CD}$, $K=699.21 \text{ M}^{-1}$ with $\beta\text{-CD}$ and $K=177 \text{ M}^{-1}$ with $\gamma\text{-CD}$ [45]. The negative free energy change ($\Delta G/\text{kJ mol}^{-1}=-22.03$, -16.34 and -12.91 for $\alpha\text{-CD}$, $\beta\text{-CD}$ and $\gamma\text{-CD}$, respectively, dictates the spontaneity of the process of HN12:CD inclusion complex formation). An unusually high binding constant for the HN12: $\alpha\text{-CD}$ complex also stands in support of the high degree of compactness in the binding.

The orientation of the probe (HN12) inside CD nanocavity was elucidated by applying medium pH variation as the actuating tool. The pH variation experiments on the absorption profile in the presence of CDs and a direct comparison of the results with those obtained under similar conditions in the absence of CDs point towards the orientation of the probe inside the nanocage. Similar response of HN12 towards medium pH in both cases indicates that the HN12:CD complex is formed in a fashion that the functional moieties (OH and CHO groups) are oriented towards outside the cavity so as to be still accessible to external agents in the medium like H^+ or OH^- ions [45].

We have also successfully demonstrated the efficiency of the selected molecular system in probing biomimetic environments of micellar systems. Micelles are one of the simplest types of organized assemblies formed from amphiphilic surfactant molecules in aqueous medium and are able to mimic biomembranes in a much simpler model. Micelles also find their association in research in the field of drug-delivery [80] because of their unique structural architecture, chemical properties and ability to act as a solubility enhancer for a wide range of feebly water-soluble pharmaceuticals [81]. Micelles thus naturally happen to form a promising and attractive platform of research. The nature of modifications in the spectral properties of HN12 upon interaction with micelles has been followed with an ionic (SDS) and a non-ionic (Tween-20) surfactant and the pattern of modulations again suggests the binding of HN12 molecules to some hydrophobic

region of the micellar assemblies and receives further verification of our proposition from steady state anisotropy and lifetime measurements. However, fluorescence quenching experiments with an ionic quencher (Cu^{2+}) indicate the location of the probe molecules at micelle–water interface (enhanced quenching of HN12 fluorescence in SDS and TW-20 media compared to that in bulk aqueous phase indicating greater proximity of the quencher to the fluorophore promoted by electrostatic attraction between Cu^{2+} ions and negative charge of SDS micelles/localized negative charge density of the heteroatoms of the head groups of TW-20 micelles). The modulation of ESIPT emission of HN12 upon action of urea on micelle-bound probe has been demonstrated to be a prospective strategy to replicate the effect of urea on complex biomacromolecules [45]. Additionally, the subtle difference in mode and extent of interaction of HN12 with ionic (SDS) and non-ionic (TW-20) micelles is also manifested through differential binding constants, response to the presence of urea and time-resolved measurements [45]. The estimated binding constants of HN12 with the studied micellar systems were as follows: $K=0.37 \times 10^5 \text{ M}^{-1}$ with SDS and $K=31.14 \times 10^5 \text{ M}^{-1}$ with TW-20 [45] (concurrently, the spontaneity of interaction between HN12 and the studied micellar systems is unveiled from negative free energy change of interaction, e.g., $\Delta G/\text{kJ mol}^{-1}=-26.24$ with SDS and -38.68 with TW-20). Relatively weaker binding between HN12 and the ionic micelle SDS seems to stem from the fact that all the heteroatoms of the probe are endowed with partial

negative charge (as found from DFT/B3LYP/6-31G** theoretical calculation [41]), which are expected to experience a repulsive impulse from the negatively charged SDS micellar units [45].

3.3. Photophysics and dynamics of HN12 in liposome membranes

Supramolecular chemistry has traditionally remained deeply connected to the problems of structure and stability of various macromolecules and noncovalent structural architectures such as DNA, proteins, membranes which form the fundamental units of living systems on the planet [82]. One of the most important supramolecular structures is the vesicles which are dynamical structures composed of amphiphiles forming bilayers that enclose a small amount of water within [82,83]. Vesicles, because of very obvious attractive structural architecture, have been at the focus of research over the years. More particularly, the synthetic vesicles have captured special attention on account of their efficient ability to mimic biological membranes [84,85]. Vesicles, which are composed of natural phospholipids, are termed “liposomes” which serve as models for biological membranes. Phospholipid bilayers constitute the matrix of natural membranes on which proteins, enzymes and drugs display their activities [86]. The complicated structure of natural biological membranes has always invited research in line of using synthetic liposome that mimic the structure and geometry of cell membranes [82–85]. Apart from this, the diversity of application of liposome also extends to the fields of drug loading, food industry and immunology. This section deals with recounting the interactions of HN12 with liposomal membranes having varying surface charges. Liposomal vesicles (Scheme 2) of dimyristoyl- $\text{l}-\alpha$ -phosphatidylcholine (DMPC) and dimyristoyl- $\text{l}-\alpha$ -phosphatidylglycerol (DMPG) have been used for the purpose.

The absorption spectra of HN12 are found to be hardly modified by the presence of lipids except for slight increase in absorbance with increasing lipid concentration. On the contrary, the results of interaction of HN12 with DMPC and DMPG lipid-bilayers are more dramatically reflected on the emission profile. Fig. 11 shows remarkable intensity enhancement of both the rotamer (open form) ($\lambda_{\text{em}} \sim 350 \text{ nm}$) and the tautomer (K-form) ($\lambda_{\text{em}} \sim 480 \text{ nm}$) emission of HN12 with increasing lipid concentration (DMPC and DMPG). The extent of modulation is found to be comparatively greater for the tautomer emission than the rotamer emission, and the effect is even more prominently seen in DMPG lipid compared to DMPC. A close inspection of Fig. 11 also reveals a slight blue shift of the emission maxima upon interaction with the lipids ($\Delta\lambda_{\text{em}}^{\text{max}} \sim 5 \text{ nm}$). The higher fluorescence quantum yield of HN12 in aprotic medium ($\Phi_f=0.014$ in cyclohexane) compared to that in protic medium ($\Phi_f=0.007$ in water) combined with the relative emission maxima positions ($\lambda_{\text{em}}^{\text{max}} \sim 475 \text{ nm}$ in cyclohexane vs. $\lambda_{\text{em}}^{\text{max}} \sim 480 \text{ nm}$ in water) [44] produces clues to assess the nature and mechanism of interactions responsible for the observed modifications on the emission spectral profile of HN12 [42–45]. A slight blue shift coupled with fluorescence quantum yield enhancement (Φ_f of HN12 increases to 0.022 and 0.034 in 1.0 mM DMPC and DMPG, respectively [44]) in lipid environments indicates that the polarity around the lipid-bound fluorophore is less than that in bulk aqueous phase (buffer medium). The blue shift is, however, not very large because of an intrinsic “intramolecular” nature of the ESIPT phenomenon whence the emission properties (particularly $\lambda_{\text{em}}^{\text{max}}$ position) of the external probe exhibit negligible medium-polarity dependence.

A quantitative assessment of the emission spectral modulations of HN12 upon interaction with the lipids has been framed following the method described by Rodrigues et al. [86], in order to delve into the ability of the molecular probe to partition from aqueous buffer phase to the lipid environments. The partition coefficient of the

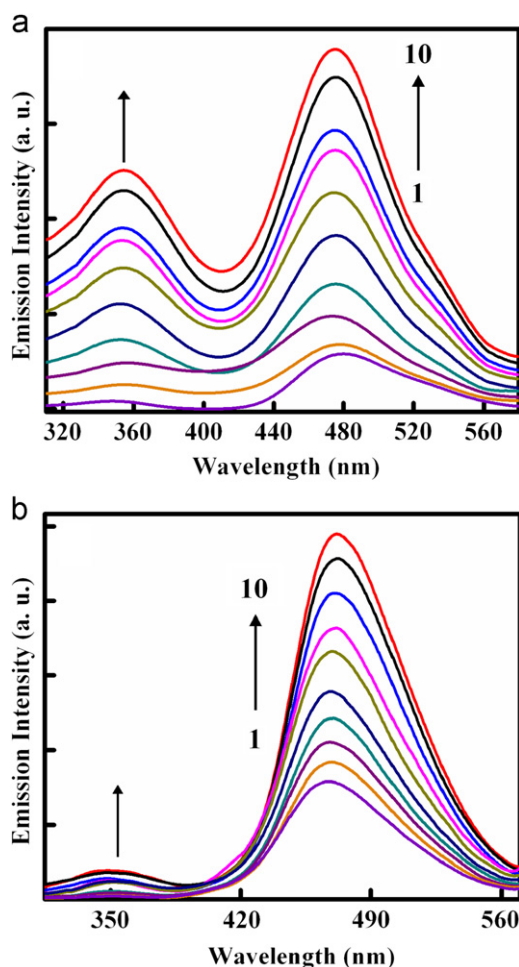


Fig. 11. Emission spectra of HN12 as a function of increasing lipid concentration ($\lambda_{\text{ex}}=300 \text{ nm}$). (a) Curves 1→10 correspond to $[\text{DMPC}]=0.0, 0.02, 0.05, 0.09, 0.30, 0.50, 0.70, 0.90, 1.50, 2.0 \text{ mM}$. (b) Curves 1→10 correspond to $[\text{DMPG}]=0.0, 0.02, 0.05, 0.09, 0.15, 0.25, 0.50, 0.80, 1.50, 2.0 \text{ mM}$.

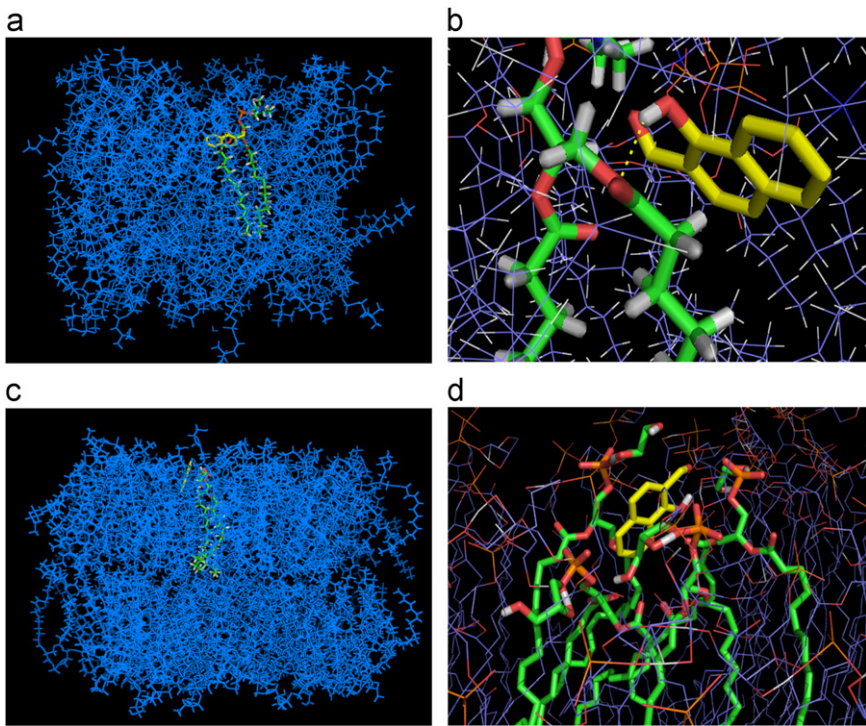


Fig. 12. Docked conformations of HN12 with the studied lipid systems. (a) Docked pose of HN12 with DMPC lipid-bilayer, (b) magnified view of the site of interaction of HN12 with DMPC. (c) Docked pose of HN12 with DMPG lipid-bilayer, (d) magnified view of the site of interaction of HN12 with DMPG.

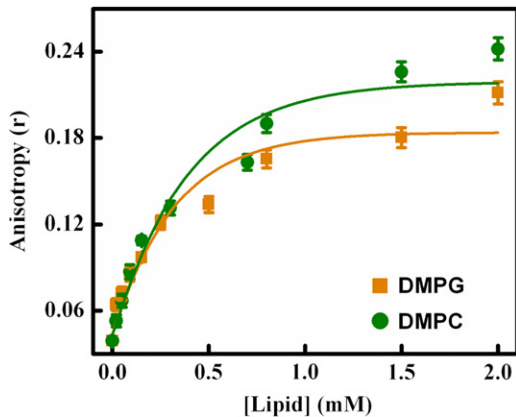


Fig. 13. Variation of steady-state fluorescence anisotropy (r) as a function of lipid concentration as specified in the figure legend ($\lambda_{\text{ex}}=300 \text{ nm}$ and $\lambda_{\text{monitored}}=\lambda_{\text{em}}^{\max}$). Each data point is an average of ten individual measurements. Error bars are within the symbols if not apparent. The solid line is merely a visual guide to indicate the pattern of variation.

probe is defined as follows [86]:

$$K_p = \frac{(C_m/C_t)/[\text{Lipid}]}{(C_w/C_t)/[\text{Water}]} \quad (3)$$

where C_t is the total molar concentration of the probe, C_m and C_w stand for probes in lipid (DMPC or DMPG) and in water, respectively. Terms within square brackets represent molar concentration of respective species. The experimentally obtained partition coefficient values are $K_p=(5.99 \pm 1) \times 10^4$ in DMPC and $K_p=(2.32 \pm 1) \times 10^5$ in DMPG [44]. Such high magnitudes of K_p are, indeed, a clear manifestation of efficient partitioning of the probe in liposome membranes. Apart from being consensus with literature reports [82,87–90], the K_p values indicate greater partitioning of the probe in anionic DMPG membrane compared to that in zwitterionic DMPC membrane. This is further corroborated from the results of docking

simulation (as performed with AutoDock 4.2 software package [91,92]). A lower magnitude of inhibition constant for binding interaction of HN12 with DMPG lipid-bilayer compared to that with DMPC ($516.01 \mu\text{M}$ in DMPG vs. $722.83 \mu\text{M}$ in DMPC) substantiates the higher K_p with DMPG lipid [44]. Furthermore, the results of docking simulation studies reveal the probable binding location of the probe in the lipids. The results displayed in Fig. 12 unveil that the preferred conformation of HN12 with favorable binding interaction is achieved when HN12 is located in the head-group region of the lipid-bilayers [44].

The steady-state fluorescence anisotropy measurements also reflect the interaction of HN12 with the lipid systems. The anisotropy value is found to be considerably increased with increasing lipid concentration indicating the impartation of motional rigidity to the molecular probe (Fig. 13). Attainment of a plateau region in Fig. 13 implies saturation in the interaction between the two parties. An increase in the anisotropy value of HN12 in DMPG lipid environment is relatively greater than that in DMPC lipid, at the same concentration of the probe and the lipid (Fig. 13). This finding is a nice corroboration to the stronger binding interaction of the probe with DMPG as compared to DMPC lipid and is consistent with the results discussed previously.

Like the steady-state spectroscopic response of HN12, the dynamic behaviors of the probe were also enormously modified within the lipid environments. The fluorescence lifetime of the probe was found to be steadily enhanced with increasing lipid concentration which was due to diminution of nonradiative decay channels through reduction of rotational/vibrational degrees of freedom resulting from its encapsulated state in the lipid environments. In order to further construe the modulations in excited state behavior of HN12 we have calculated the radiative (k_r) and nonradiative (k_{nr}) decay rate constants using the following two equations [93]:

$$k_r = \frac{\Phi_f}{\langle \tau_f \rangle} \quad (4)$$

Table 2

Time-resolved fluorescence decay parameters, quantum efficiency and radiative and non-radiative decay rate constants of HN12 in lipids.

Environment	$\tau_1/\text{ns} (\alpha_1)$	$\tau_2/\text{ns} (\alpha_2)$	$\tau_3/\text{ns} (\alpha_3)$	$\langle \tau_f \rangle/\text{ns}$	χ^2	Φ_f^{a}	$k_r \times 10^{-7} (\text{s}^{-1})$	$k_{\text{nr}} \times 10^{-9} (\text{s}^{-1})$
Aqueous buffer	0.087 (0.91)	0.588 (0.09)	–	0.287	1.50	0.007	2.433	3.459
0.5 mM DMPC	0.701 (0.031)	3.228 (0.001)	0.062 (0.967)	0.348	1.19	0.011	3.161	2.842
1.0 mM DMPC	0.517 (0.035)	2.021 (0.0363)	0.544 (0.929)	1.131	1.02	0.022	1.945	0.865
1.5 mM DMPC	0.531 (0.039)	1.975 (0.042)	0.0509 (0.92)	1.174	1.13	0.033	2.811	0.824
0.5 mM DMPG	0.731 (0.024)	2.961 (0.0099)	0.0543 (0.966)	1.031	1.09	0.012	1.164	0.958
1.0 mM DMPG	1.362 (0.053)	3.928 (0.0086)	0.055 (0.783)	1.562	1.19	0.034	2.177	0.618
1.5 mM DMPG	1.573 (0.079)	6.237 (0.0045)	0.052 (0.917)	2.074	1.19	0.056	2.7	0.455

^a Quantum yields are calculated with anthracene as the secondary standard [44,45].

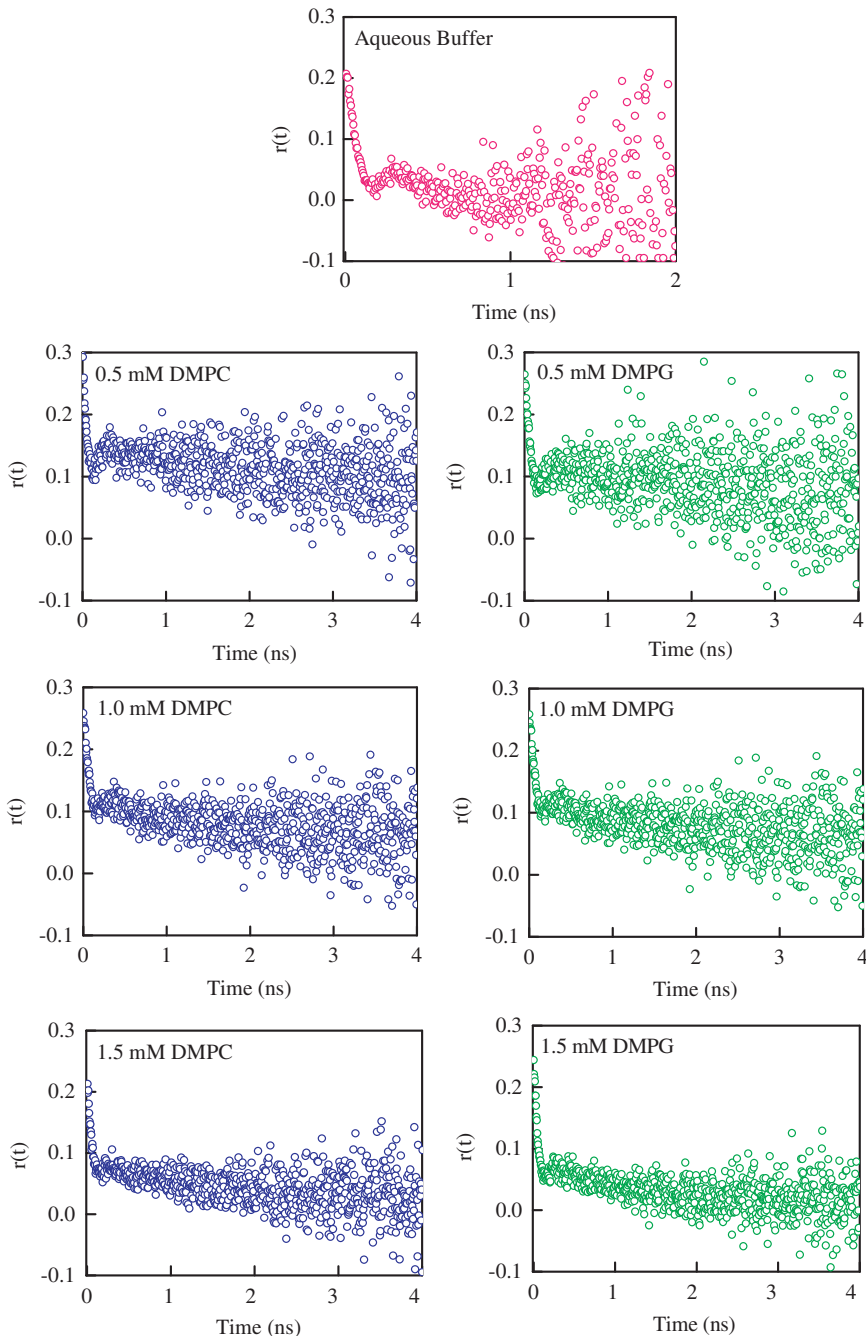


Fig. 14. Time-resolved fluorescence anisotropy decay profile of HN12 in various lipid environments as indicated in the figure legend ($\lambda_{\text{ex}}=375 \text{ nm}$ and $\lambda_{\text{monitored}}=\lambda_{\text{em}}^{\text{max}}$).

$$k_{\text{nr}} = \frac{1}{\langle \tau_f \rangle} - k_r \quad (5)$$

Here, Φ_f is the fluorescence quantum efficiency and $\langle \tau_f \rangle$ is the average fluorescence lifetime. Calculations suggest that the radiationless decay rates are considerably reduced in lipid

environments compared to that in bulk aqueous buffer medium (Table 2) whereby substantiating our previous assignments [42–45,92].

However, more intriguing to note is the modulation of fluorescence anisotropy decay kinetics of HN12 within lipid environments. The typical anisotropy decay profile of HN12 in aqueous buffer as well as lipid environments is presented in Fig. 14. It is, indeed, surprising to note that the probe exhibited an unusual “dip-and-rise” pattern in the fluorescence anisotropy decay in aqueous buffer solution with the prominence of the specific dip-and-rise pattern being progressively obscured with increasing lipid concentration. Such dip-and-rise kind of profile is a signature for the juxtaposition of at least two populations, one with a short fluorescence lifetime and a short rotational correlation time and another having both the time constants longer compared to those of the first population [93–97]. This sort of anisotropy decay behavior has been described as associated anisotropy by Lakowicz [93] and has been previously observed in several situations [93–97]. However, usually this kind of anisotropy decay profile has been observed for fluorophores in confined environments in which the faster motion is attributed to the solvent exposed groups/moieties of the fluorophore and the slower motion to the bound counterpart, with the usual trend that the appearance of the “dip-and-rise” pattern is rendered more prominent with increasing degree of confinement [93–97]. It was initially quite puzzling for us to note a qualitatively reverse trend (with respect to usual reports found in the literature [93–97]) in the present findings in the form that the dip-and-rise pattern is more prominently seen for HN12 in bulk aqueous buffer phase while it is gradually obscured with increasing lipid concentration. It is argued that this type of anisotropy decay profile is best obtained when the two lifetime values are significantly different [93–97]. This prerequisite is evidently satisfied for HN12 in aqueous buffer phase, as can be seen in Table 2. Now, at this stage it is not unlikely if we consider the origin of the dip-and-rise pattern of fluorescence anisotropy decay of HN12 in aqueous buffer phase to be emanating from contributions from the PT form of HN12 and the solvated structure. This is obvious that the population of the solvated structure of HN12 will be progressively discouraged with increasing lipid concentration, whereby resulting in obscuring the appearance of the dip-and-rise pattern in the anisotropy decay profiles (Fig. 14). Clearly, interplay between different intramolecular and intermolecular motions is being invoked here to account for the observed anisotropy decay profile. Therefore, modulations of these motions upon interaction with the liposome membranes should naturally contribute in governing the overall motional dynamics of the probe within the lipid environments. However, with a view to the observation of enhancement of the average fluorescence lifetime of HN12 upon binding to the lipids and the possibility of coupling of the motions of the probe with global tumbling motion of the liposome units, the internal motions of the probe cannot be considered as the sole criterion for generating the dip-and-rise anisotropy profile [93–97].

One major utility of time-resolved anisotropy decay measurements is associated with the application in evaluation of the binding site of the probe through the calculation of the generalized order parameter (S) in the course of monitoring the rotational relaxation dynamics of a fluorophore in an organized medium [44,98–102]. For this purpose, we fitted the anisotropy decay curves for HN12 in the presence of a substantial lipid concentration ([Lipid]=1.5 mM) with two rotations only (one fast and another slower rotation). The fitted parameters are as follows: for HN12 in 1.5 mM DMPC the two rotational relaxation times are $\theta_1=34$ ps ($\alpha_{1r}=0.74$) and $\theta_2=1.62$ ns ($\alpha_{2r}=0.26$) with $\chi^2=1.21$ and for HN12 in 1.5 mM DMPG the values are $\theta_1=33$ ps ($\alpha_{1r}=0.75$) and $\theta_2=1.25$ ns ($\alpha_{2r}=0.25$) with $\chi^2=1.25$.

The order parameter (S), as defined as $S^2=\alpha_{2r}$, provides information about the motional restrictions on the probe molecule. It is a measure of the spatial restriction having values ranging from 0 (corresponding to unrestricted motion) to 1 (for complete restriction on the motion) [44,98–102]. The calculated values for the order parameter are $S=0.51$ in DMPC and 0.50 in DMPG lipid. Such reasonably high magnitude of the order parameter suggests the binding site of the probe to be in the lipid head-group region. From NMR relaxation data [98,99] and other experimental techniques [100–102] it has been documented that there is higher degree of order near the surface than in the interior of liposome systems. In fact, in the hydrocarbon interior of the liposomes the order parameter is known to be enormously low, since the wobbling motion of the probe is expected to be almost isotropic [44,98–102].

3.4. Wavelength-sensitive fluorescence behavior of HN12: the red-edge excitation

It was almost four decades ago when three laboratories independently reported an unusual spectroscopic behavior of organic fluorophores in rigid and highly viscous environment. W. Galley in Canada [103] and Rubinov in Belarus [104] demonstrated that fluorescence spectra recorded in low-temperature glasses shift to longer wavelengths upon excitation at the long wavelength slope, ‘the red-edge’, of the absorption spectrum. At the same time, Weber made a generalization of his earlier discovery [105] that

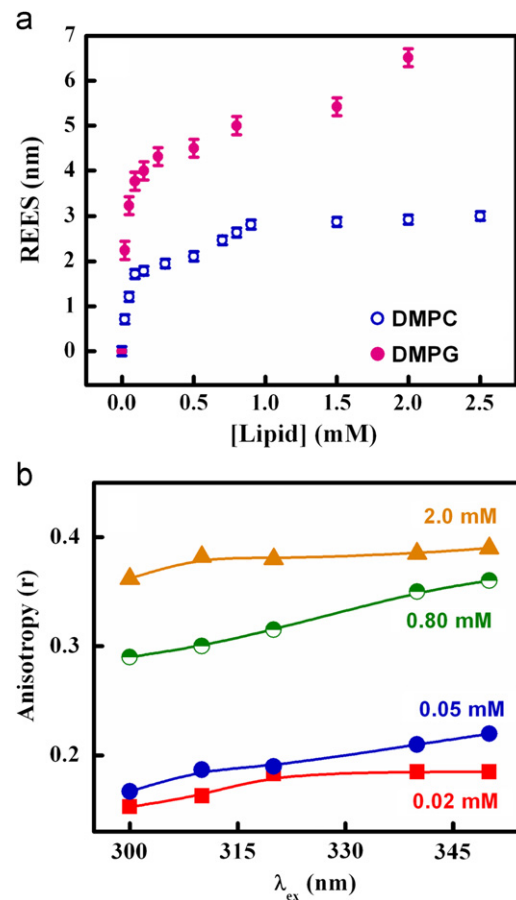


Fig. 15. (a) Representative REES spectra for HN12 in different lipid environments. Plot of REES ($\Delta\lambda_{\text{ex}}^{\text{max}}$ in nm) with increasing lipid concentration (mentioned in the figure legend) for variation of excitation wavelength from $\lambda_{\text{ex}}=370$ nm → 430 nm for each data point. Error bars are within the symbols if not apparent. (b) Representative excitation anisotropy profile for HN12 in DMPC lipids at some specified DMPC concentrations indicated in the figure legend.

excited-state energy homotransfer, if it exists, vanishes at the red-edge excitation. However, these findings were contrary to the commonly accepted concepts of independence of emission energy on excitation energy within the absorption band (Vavilov's law) and the occurrence of emission, irrespective of excitation band, always from the lowest electronic and vibrational state of the same multiplicity (Kasha's rule) [106]. Since the discovery of this phenomenon, well known as "red-edge excitation shift" (REES), it continues to be exploited quite extensively by several research groups for studies in biological and biomimicking systems [107–109]. Here we decipher the commendable sensitivity of HN12 towards furnishing valuable information about the micero-heterogeneous environments of various organized assemblies through exploration of REES effects. Fig. 15a depicts the red-edge effect of HN12 in presence of liposomal membranes (DMPC and DMPG) reflecting the variation of its microenvironment with lipid concentration. Also a similar observation of a more or less linear increase of anisotropy (Fig. 15b) adds further strength to our interpretation of the results in terms of increasing motional restrictions [53–55]. These phenomena have been noted in other organized media (protein, CDs, micelles) also [42–45]. However, with a view to reasonably longer lifetime of HN12 in motionally restricted media [42–45], it seems reasonable to propose that the observed REES in the studied organized media is not due to fluorescence from an unsolvated (or partially solvated, and hence incompletely relaxed) state [110,111], rather fluorescence occurs from fully solvated state in these systems since the excited state fluorescence life-times may be longer than (or comparable to) the solvent relaxation time. Rather some other sort of mechanism (something other than slow solvation) seems to play the pivotal role in creating a distribution of energetically different molecules in the ground state that allows their photoselection [107–111] and we propose that different types of hydrogen bonding interaction and their perturbations or modifications to different extents under different complex environments (provided by CD nanocavities, micellar media, proteins and lipids) might play a role in producing ground state inhomogeneity and thereby allowing initial photo-selection. Though to be very particular about the reason stated above is not quite easy given the inherently complex nature of hydrogen bonding interaction and also the complexity provided by the organized assemblies [44]. Presently investigations are underway in our laboratory to pinpoint on the issue.

4. Summary and conclusion

The wealth of information available for the ESIPT reaction of prototype molecule methylsalicylate (MS) and related compounds is somewhat contrasted by the lack of similar data on their corresponding naphthalene analogs. This account deals with the recollection of the rich spectroscopy and dynamics of a comparatively simple aromatic molecule, 1-hydroxy-2-naphthaldehyde (HN12) bearing two H-bonding groups (OH and CHO) which, following photoexcitation, reach an electronic state having the proton exchanged across an already existing IMHB at the ground state. Theoretical work is found to strongly support and complement the experimental observations for the occurrence of ESIPT in HN12. Unlike the medium polarity, the variation of medium pH and temperature are found to exert profound modifications to the ground and excited state photophysics of HN12. The series of spectroscopic work carried out with HN12 establishes the candidature of HN12 as a sensitive and efficient fluorescent reporter for a wide range of supramolecular, biomimicking and biological microenvironments through exploitation of its ESIPT phenomenon, and simultaneously advocates for its promising future applications.

We are optimistic that the results and conclusions derived from the studies of HN12, apart from the theoretical work, will deliver positive impact towards a better understanding of the behavior of several molecular systems undergoing this kind of phenomena. ESIPT reaction across a pre-existing IMHB is also pertinent to key reactions occurring in many biological systems.

Acknowledgments

BKP is grateful to CSIR, New Delhi, India, for research fellowship. NG acknowledges CSIR and DST, Government of India, for financial assistance.

References

- [1] A.H. Weller, Fast reactions of excited molecules, *Prog. React. Kinet.* 1 (1961) 187.
- [2] A.R. Morales, K.J. Schafer-Hales, C.O. Yanez, M.V. Bondar, O.V. Przhonska, A.I. Marcus, K.D. Belfield, *Chem. Phys. Chem.* 10 (2009) 2073–2081.
- [3] H. Ishikawa, K. Iwata, H. Hamaguchi, *J. Phys. Chem. A* 106 (2002) 2305.
- [4] B.K. Paul, A. Samanta, N. Guchhait, *Photochem. Photobiol. Sci.* 9 (2010) 57.
- [5] E. Lippert, W. Luder, H. Boos, in: A. Mangini (Ed.), *Advances in Molecular Spectroscopy*, Pergamon Press, Oxford, 1962, p. 443.
- [6] A. Chakraborty, S. Kar, D.N. Nath, N. Guchhait, *J. Phys. Chem. A* 110 (2006) 12089.
- [7] I. Gomez, M. Reguero, M. Boggio-Pasqua, M.A. Robb, *J. Am. Chem. Soc.* 127 (2005) 7119.
- [8] B.K. Paul, A. Samanta, S. Kar, N. Guchhait, *J. Luminesc.* 130 (2010) 1258.
- [9] L. Fajari, P. Fors, K. Lang, S. Nonell, F.R. Trull, *J. Photochem. Photobiol. A* 93 (1996) 119.
- [10] J.D. Simon, *Acc. Chem. Res.* 21 (1988) 128.
- [11] L. Banares, A.A. Heikal, A. Zewail, *J. Phys. Chem.* 96 (1992) 4127.
- [12] I.L. Finar, 6th ed., *Organic Chemistry*, vol. 1, Pearson Education (Singapore) Pte. Ltd., Indian Branch, 2003.
- [13] J. Förster, *Ann. Phys. (Leipzig)* 2 (1948) 55.
- [14] X. Li, M. McCarroll, P. Kohli, *Langmuir* 22 (2006) 8615.
- [15] B.K. Paul, A. Samanta, N. Guchhait, *J. Phys. Chem. A* 114 (2010) 6097.
- [16] A. Ajayaghosh, C. Vijayakumar, V.K. Praveen, S.S. Babu, R. Varghese, *J. Am. Chem. Soc.* 128 (2006) 7174.
- [17] R.B. Singh, S. Mahanta, N. Guchhait, *Chem. Phys.* 331 (2007) 189.
- [18] S. Mahanta, R.B. Singh, D. Nath, N. Guchhait, *J. Photochem. Photobiol. A* 197 (2008) 62.
- [19] B.K. Paul, A. Samanta, N. Guchhait, *J. Fluoresc.* 21 (2011) 1265.
- [20] B.K. Paul, A. Samanta, S. Kar, N. Guchhait, *J. Photochem. Photobiol. A: Chem.* 214 (2010) 203.
- [21] S. Maheshwary, A. Chowdhury, N. Sathyamurthy, H. Mishra, H.B. Tripathi, M. Panda, J. Chandrasekhar, *J. Phys. Chem. A* 103 (1999) 6257.
- [22] B.K. Paul, S. Mahanta, R.B. Singh, N. Guchhait, *J. Phys. Chem. A* 114 (2010) 2618.
- [23] N. Agmon, *J. Phys. Chem. A* 109 (2005) 13.
- [24] K. Sakota, H. Sekiya, *J. Phys. Chem. A* 109 (2005) 2722.
- [25] P.B. Bish, M. Okamoto, S. Hirayama, *J. Phys. Chem. B* 101 (1997) 8850.
- [26] A.L. Sobolewski, W. Domcke, *Phys. Chem. Chem. Phys.* 8 (2006) 3410.
- [27] J. Catalán, J.C. del Valle, *J. Am. Chem. Soc.* 115 (1993) 4321.
- [28] B.K. Paul, A. Samanta, N. Guchhait, *J. Mol. Struct.* 977 (2010) 78.
- [29] H.J. Heller, H.R. Blattmann, *Pure Appl. Chem.* 36 (1973) 141.
- [30] P.T. Chou, M.L. Martinez, J.H. Clements, *Chem. Phys. Lett.* 204 (1993) 395.
- [31] P.T. Chou, D. MxMorrow, T.J. Aartsma, M. Kasha, *J. Phys. Chem.* 88 (1984) 4596.
- [32] M.E. Balmer, H.-R. Buser, M.D. Muller, T. Poiger, *Environ. Sci. Technol.* 39 (2005) 953.
- [33] S. Panja, P. Chowdhury, S. Chakravorti, *Chem. Phys. Lett.* 368 (2003) 654.
- [34] K. Sahu, D. Roy, S.K. Mondal, R. Karmakar, K. Bhattacharyya, *Chem. Phys. Lett.* 404 (2005) 341.
- [35] S. Sutton, N.L. Campbell, A.I. Cooper, M. Kirkland, W.J. Frith, D.J. Adams, *Langmuir* 25 (2009) 10285.
- [36] B. Cohen, D. Huppert, K.M. Solntsev, Y. Tsafadia, E. Nachliel, M. Gutman, *J. Am. Chem. Soc.* 124 (2002) 7539.
- [37] E.L. Roberts, P.T. Chou, T.A. Alexander, R.A. Agbaria, I.M. Warner, *J. Phys. Chem.* 99 (1995) 5431.
- [38] A. Banerjee, E. Mikhaillova, S. Cheley, L.-Q. Gu, M. Montoya, Y. Nagaoaka, E. Gouaux, H. Bayley, *Proc. Natl. Acad. Sci. USA* 107 (2010) 8165.
- [39] A. Douhal, *Chem. Rev.* 104 (2004) 1955.
- [40] S. Mondal, S. Basu, D. Mandal, *Chem. Phys. Lett.* 479 (2009) 218.
- [41] R.B. Singh, S. Mahanta, S. Kar, N. Guchhait, *Chem. Phys.* 331 (2007) 373.
- [42] R.B. Singh, S. Mahanta, N. Guchhait, *J. Photochem. Photobiol. B* 91 (2008) 1.
- [43] R.B. Singh, S. Mahanta, N. Guchhait, *Chem. Phys. Lett.* 463 (2008) 183.
- [44] B.K. Paul, N. Guchhait, *J. Phys. Chem. B* 114 (2010) 12528.
- [45] B.K. Paul, A. Samanta, N. Guchhait, *Langmuir* 26 (2010) 3214.
- [46] D.-L. Wu, L. Liu, G.-F. Liu, D.-Z. Jia, *J. Phys. Chem. A* 111 (2007) 5244.

- [47] R. de Vivie-Riedle, V.D. Waele, L. Kurtz, E. Riedle, *J. Phys. Chem. A* 107 (2003) 10591.
- [48] A.E. Shchavlev, A.N. Pankratov, A.V. Shalabay, *J. Phys. Chem. A* 109 (2005) 4137.
- [49] S.-I. Nagaoka, J. Kusunoki, T. Fujibuchi, S. Hatakenaka, K. Mukai, U. Nagashima, *J. Photochem. Photobiol. A: Chem.* 122 (1999) 151.
- [50] B.A. Zhadorozhnyi, I.K. Ishchenko, *Opt. Spectrosc. (Engl. Transl.)* 19 (1965) 306–308.
- [51] R.M. Badger, *J. Chem. Phys.* 8 (1940) 288.
- [52] S. Tobita, M. Yamamoto, N. Kurahayashi, R. Tsukaghoshi, Y. Nakamura, H. Shizuka, *J. Phys. Chem. A* 102 (1998) 5206.
- [53] B.K. Paul, N. Guchhait, *J. Colloid Interface Sci.* 353 (2011) 237.
- [54] R. Das, S. Mitra, D. Nath, S. Mukherjee, *J. Phys. Chem.* 100 (1996) 14514.
- [55] J. Kang, Y. Liu, M.-X. Xie, S. Li, M. Jiang, Y.-D. Wang, *Biochim. Biophys. Acta* 2004 (1674) 205.
- [56] A. Sytnik, J.C.D. Valle, *J. Phys. Chem.* 99 (1995) 13028.
- [57] A.S. Klymchenko, V.G. Pivovarenko, A.P. Demchenko, *J. Phys. Chem. A* 107 (2003) 4211.
- [58] J. Zhao, S. Ji, Y. Chen, H. Guo, P. Yang, *Phys. Chem. Chem. Phys.* (2012) <http://dx.doi.org/10.1039/C2CP23144A>, and references therein.
- [59] G.A. Brucker, T.C. Swinney, D.F. Kelley, *J. Phys. Chem.* 95 (1991) 3190.
- [60] T.C. Swinney, D.F. Kelley, *J. Phys. Chem.* 95 (1991) 10369.
- [61] T. Elsaesser, B. Schmetzler, *Chem. Phys. Lett.* 140 (1987) 293.
- [62] C.A.S. Potter, R.G. Brown, *Chem. Phys. Lett.* 153 (1988) 7.
- [63] S. Sugio, A. Kashima, S. Mochizuki, M. Noda, K. Kobayashi, *Protein Eng.* 12 (1999) 439.
- [64] G.M. Morris, D.S. Goodsell, R.S. Halliday, R. Huey, W.E. Hart, R.K. Belew, A.J. Olson, *J. Comput. Chem.* 19 (1998) 1639 and references therein.
- [65] H. Park, O. Chi, J. Kim, S. Hong, *J. Chem. Inf. Model.* 51 (2011) 2985.
- [66] C. Hetenyi, D. van der Spoel, *FEBS Lett.* 580 (2006) 1447.
- [67] S.W. Homan, *Top. Curr. Chem.* 272 (2007) 51.
- [68] B.K. Paul, D. Ray, N. Guchhait, *Phys. Chem. Chem. Phys.*, <http://dx.doi.org/10.1039/c2cp23496c>.
- [69] B.K. Paul, N. Guchhait, *J. Phys. Chem. B* 115 (2011) 10322.
- [70] Y. Moriyama, K. Takeda, *Langmuir* 15 (1999) 2003.
- [71] Y. Moriyama, K. Takeda, *Langmuir* 21 (2005) 5524.
- [72] S. Deep, J.C. Ahluwalia, *Phys. Chem. Chem. Phys.* 3 (2001) 4583.
- [73] D.E. Otzen, *Biophys. J.* 83 (2002) 2219.
- [74] N.K. Zaitsev, I.I. Kulakov, M.G. Kuzmin, *Sov. Electrochem. (Engl. Ed.)* 21 (1985) 1293.
- [75] E.L. Gelano, C.H.T.P. Silva, H. Imasato, M. Tabak, *Biochim. Biophys. Acta* 1594 (2002) 84.
- [76] W. Saenger, *Angew. Chem. Int. Ed. Engl.* 19 (1984) 344.
- [77] R. Villalonga, R. Cao, A. Fragoso, *Chem. Rev.* 107 (2007) 3088.
- [78] K. Ukama, F. Hirayama, T. Irie, *Chem. Rev.* 98 (1998) 2045.
- [79] S. Li, W.C. Purdy, *Chem. Rev.* 92 (1992) 1457.
- [80] A. Muller, D.F. O'Brien, *Chem. Rev.* 102 (2002) 727.
- [81] Z. Geo, A.N. Lukyanov, A. Singhal, V.P. Torchilin, *Nano Lett.* 2 (2002) 979.
- [82] J. Voskuhl, B.J. Ravoo, *Chem. Soc. Rev.* 38 (2008) 495.
- [83] J.F. Nagle, S. Tristram-Nagle, *Biochim. Biophys. Acta* 1469 (2000) 159–195.
- [84] N. Ashgarian, Z.A. Schelly, *Biochim. Biophys. Acta* 1418 (1999) 295.
- [85] F. Moyano, M.A. Biasutti, J.J. Silber, J.J. Correa, *J. Phys. Chem. B* 110 (2006) 11838.
- [86] C. Rodrigues, P. Gamerio, S. Reis, J.L.F.C. Lima, B.D. Castro, *Langmuir* 18 (2002) 10231.
- [87] J. Sujatha, A.K. Mishra, *Langmuir* 14 (1998) 2256.
- [88] A. Kyrychenko, F. Wu, R.P. Thummel, J. Waluk, A.S. Ladokhin, *J. Phys. Chem. B* 114 (2010) 13574.
- [89] S. Chaudhuri, B. Pahari, P.K. Sengupta, *Biophys. Chem.* 139 (2009) 29.
- [90] M. Halder, P. Mukherjee, S. Bose, M.S. Hargrove, X. Song, J.W. Petrich, *J. Chem. Phys.* 127 (2007) 55101.
- [91] G.M. Morris, D.S. Goodsell, R.S. Halliday, R. Huey, W.E. Hart, R.K. Belew, A.J. Olson, *J. Comput. Chem.* 19 (1998) 1639.
- [92] G.M. Morris, R. Huey, W. Lindstrom, M.F. Sanner, R.K. Belew, D.S. Goodsell, A.J. Olson, *J. Comput. Chem.* 30 (2009) 2785.
- [93] J.R. Lakowicz, *Principles of Fluorescence Spectroscopy*, Plenum, New York, 1999.
- [94] D. Banerjee, S.K. Srivastava, S.K. Pal, *J. Phys. Chem. B* 112 (2008) 1828.
- [95] O.K. Abou-Zied, O.I.K. Al-Shibli, J. Am. Chem. Soc. 130 (2008) 10793.
- [96] C.W. Ko, Z. Wei, R.J. Marsh, D.A. Armoogum, N. Nicolaou, A.J. Bain, A. Zhou, L. Ying, *Mol. BioSyst.* 5 (2009) 1025.
- [97] A. Jha, J.B. Udgaoarkar, G. Krishnamoorthy, *J. Mol. Biol.* 393 (2009) 735.
- [98] H. Nery, O. Smerman, D. Canet, H. Walderhaug, B. Lindman, *J. Phys. Chem.* 90 (1986) 5802.
- [99] J. Mascetti, S. Castano, D. Cavagnat, B. Desbat, *Langmuir* 24 (2008) 9616.
- [100] S. Thirunavukkaran, E.A. Jares-Erijman, T.M. Jovin, *J. Mol. Biol.* 378 (2008) 1064.
- [101] S. Dutta Choudhury, M. Kumbhakar, S. Nath, H. Pal, *J. Chem. Phys.* 127 (2007) 194901.
- [102] J. Yang, R.S. Roller, M.A. Winnik, *J. Phys. Chem. B* 110 (2006) 11739.
- [103] W.C. Galley, R.M. Purkey, *Proc. Natl. Acad. Sci. USA* 67 (1970) 1116.
- [104] A.N. Rubinov, V.I. Tomin, *Opt. Spektr.* 29 (1970) 1082.
- [105] G. Weber, *Biochem. J.* 75 (1960) 345.
- [106] M. Respondek, T. Madl, C. Gobl, R. Golser, K. Zanger, *J. Am. Chem. Soc.* 129 (2007) 5228.
- [107] G. Maglia, A. Jonckheer, M.D. Maeyer, J.-M. Frere, Y. Engelborghs, *Protein Sci.* 17 (2008) 352.
- [108] A. Samanta, *J. Phys. Chem. B* 110 (2006) 13704.
- [109] E.L. Roberts, J. Dey, I.M. Warner, *J. Phys. Chem. A* 101 (1997) 5296.
- [110] B.K. Paul, A. Samanta, N. Guchhait, *J. Phys. Chem. B* 114 (2010) 6183.
- [111] A.P. Demchenko, *Luminescence* 17 (2002) 19.